Beam Dynamics and Performance of a 15.6 GHz Ceramic High Power RF Generator*

A. V. Smirnov, D. Yu

DULY Research Inc., Rancho Palos Verdes, CA 90275

W. Gai, H. Wang

High Energy Physics Division, Argonne National Laboratory, Argonne, IL 60439

Abstract. Beam dynamics estimations of a 15.6GHz ceramic RF power generator have been performed for an experiment planned at the upgraded AWA facility at ANL. Theoretical maximum peak power that can be generated exceeds 100-150 MW. Analytical and numerical calculations address the following issues: 50A+ heavy beam loading in linac, slow-wave structures, coupler and damper; beam breakup and dipole mode suppression, end-to-end beam transport, and generated RF waveform and spectrum. Comparison is made with an earlier 21GHz experiment in a DULY/CERN/ANL collaboration.

INTRODUCTION

In a companion paper [1] we have presented design features of a 15.6GHz extractor/coupler and compared it to a previous 21GHz design [2,3]. Here we are considering beam dynamics and performance of the dielectric power extractor to be driven by the Argonne Wakefield Accelerator (AWA) [4]. The L-band facility is being upgraded to produce an improved-quality electron beam with up to 100nC bunches and energy up to 19MeV [5].

Let us outline here some of the parameters and effects related directly to the beam dynamics and performance of the 15.6GHz extractor: higher maximum beam currents (over 100A instead of 17.2A) raise the limit of RF power but can simultaneously enhance non-linear effect of RF losses [6] and RF breakdown, larger energy spread in both the driver linac and the extractor; heavy beam loading and collective instabilities; higher harmonic operation (12^{th} vs. 7^{th}) broadens the spectrum of the pulse generated and can diminish extractor efficiency. In addition, beam interaction with such elements as the damper, the taper, and the coupler, having trapped modes, is also of our interest.

* Work supported by DOE SBIR grant number DE-FG03-01ER83232.

CP737, *Advanced Accelerator Concepts: Eleventh Workshop,*
edited by Vitaly Yakimenko

TM_{01} OPERATING MODE FIELDS INDUCED IN THE EXTRACTOR

Table 1 gives comparative parameters of two extractors with ceramic tubes supplied by Euclid Concepts Inc. These cold parameters are calculated with an accurate analytical model that was used also to benchmark the GdfidL code [7] in frequency domain. The saturated power generated by an equidistant bunch train in a slow-wave system is the following:

$$P = \frac{\omega}{4}\frac{r}{Q}\frac{1}{|v_{gr}|}\left| I\,\Phi_b L\,\frac{1-e^{-\alpha L(1+ia_s)}}{\alpha L(1+ia_s)}\right|^2, \qquad (1)$$

where r is the TM_{0n} shunt impedance per unit length, $\Phi_b = \frac{1}{q}\int_q \frac{dq}{dz}(z')\exp\left(-i\frac{kz'}{\beta}\left(1-\frac{i/2Q}{1-\beta_{gr}/\beta}\right)\right)dz'$ is the bunch formfactor, q is the bunch charge, $\omega = 2\pi f = h(\omega)/v$ is the resonant frequency, $\beta = v/c$, $k = \omega/c$, $a_s = 2Q(f/n_h f_b - 1)(1-\beta_{gr}/\beta)$ is the generalized detuning, f_b is the bunch train frequency, $n_h = Integer(f/f_b)$ is the resonant harmonic number, L is the interaction length, and $\alpha = \pi f Q/v_{gr}$ is the attenuation constant. Formula (1) accounts for detuning and, along with the solution of boundary problem, allows to define tolerances for geometrical and material imperfections [1]. It is accurate for a given monopole mode in an arbitrary slow-wave non-tapered guide if the following is satisfied:

$$2Q\left|\beta-\beta_{gr}\right| >> 1, \quad \left[L\left(\beta_{gr}{}^{-1}-\beta^{-1}\right)f_b/c\right]^2 >> 1 \qquad (2)$$

Correspondingly, for a single bunch the maximum (peak) radiated power is the following:

$$P_{1b} = \frac{\omega}{4}\frac{r}{Q}|v_{gr}|\cdot\left|\frac{q\Phi_b}{1-\beta_{gr}/\beta}\right|^2 \qquad (3)$$

Equation (3) includes the power absorbed in the dielectric and is accurate if conditions (2) are applied, where f_b is replaced by f.

The main characteristics are calculated at $a_s << 1$ in Table 2, where t_f is the filling time for a regular dielectric length L=30cm, δ_z is the r.m.s. length assuming Gaussian bunch with the formfactor $\Phi_b \approx \exp\left(-(k\delta_z/\beta)^2/2\right)$, and N_f is the minimum number of bunches required to achieve saturation.

TABLE 1. Geometry and RF properties of regular dielectric part of the power generators.

f, GHz	material	ε	tgσ	Apert. ∅=2a, mm	OD, mm	r/Q, kΩ/m	Q	β_{gr}
21	corderite	4.72	0.0005	10	12.94	6.48	2252	0.354
15.6	forsterite	6.64	0.0005	12	15.42	5.64	2002	0.264

TABLE 2. Main performance characteristics at L=0.3m.

f, GHz	q, nC	f_b, GHz	I=q·f_b, A	δ_z, mm	t_f, ns	$N_f=[t_f \cdot f_b]$	Φ_b	P_{1b}, MW	$N>N_f$:P,MW
21	5.73	3	17.2	1	2.83	8	0.97	1.6	38.6
15.6	40	1.3	52	3	3.79	4	0.62	20	148

In our earlier 21GHz test at the CTF2, the maximum available total charge of the bunch train was limited by the extractor aperture to 275nC (i.e. q=5.7nC). The ultimate

power was therefore considerably less than that planned initially at q=10nC operation. The upgraded high-current AWA facility, along with our new 15.6 GHz design, gives an opportunity of higher output power (see Table 2) provided such effects as reflections, secondary electron emission (see [6]) and breakdown, beam transport and instabilities do not dominate or distort the performance. Because of the rapid decrease of the formfactor for higher harmonic numbers, the 12th harmonic of operation is already at the edge of operational efficiency. On the other hand, it means better suppression of higher frequency modes.

The dielectric extractor can be characterized efficiently with an analytical model in the time domain. Reflections, jitter, TM_{0n} HOMs, and group front diffusion can be included in the model [8]. Estimations made for our parameters given in Table 1 indicate that the monopole HOMs are not significant due to its much higher frequencies and very low formfactor. Estimated group front diffusion due to dispersion of group velocity is also negligible. Examples of RF envelopes and spectra of the signal modeled are depicted in Figure 1. One can see spectrum improvement at longer lengths: the main peak narrows, satellite peaks getting smaller. Bigger ratio of drain time to bunch separation gives better overlapping of wave packets radiated by individual bunches. However, too long an extractor length can be detrimental in terms of beam dynamics – beam transport and transverse stability.

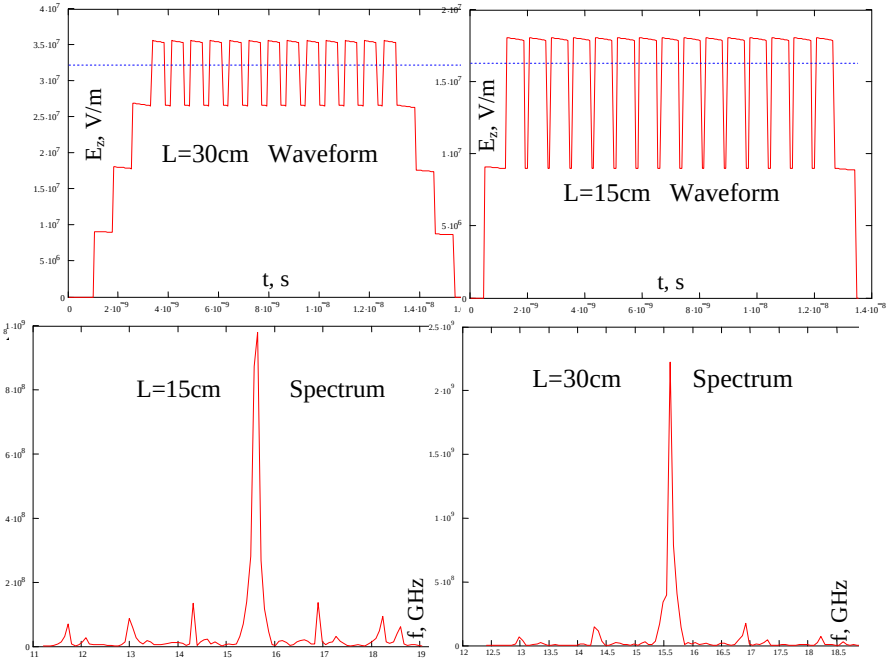

FIGURE 1. On the top: waveforms of the longitudinal field near the matched end of the dielectric tube of different lengths of regular part L. The dashed horizontal line corresponds to the formula (1). On the bottom: the corresponding field spectra. δ_z =3mm, q=40nC, number of bunches N_b=16.

From Figure 1 one can estimate the minimum bandwidth required for the coupler. Neglecting jitter and reflections the signal bandwidth is about 0.33GHz (at the level of 10%) at L=30cm.

BEAM LOADING AND OTHER WAKEFIELD EFFECTS

We distinguish several sources of energy losses: beam loading in linac cavities and regular dielectric tube, excitation of the modes trapped in the coupler, and wakefield losses in the damper and taper(s).

Let us estimate the transient beam loading (stored energy mode) in the two-section SW driver linac fed by 10+10MW RF power. The shunt impedance per section is 10.26MΩ (including transit-time factor) and unloaded Q-factor is 16860 as it is defined from preliminary Superfish calculations. Energy gain of the first q=40nC bunch is 20.06MeV, whereas the last bunch of the 20ns pulse gains only 14.9MeV. We assumed here nearly critical coupling and neglected phase detuning caused by beam loading in the first cavity of the photoinjector.

Comparable energy losses occur in the regular part of dielectric tube. In Table 3 we defined energy losses assuming Nbunches≥N_f for different lengths of the bunch and dielectric.

TABLE 3. Kinetic energy loss of trailing bunches and radiated power at saturation in the regular dielectric tube

Dielectric L regular, m	q, nC	σ_z=2mm (Δt_b=6.7ps)		σ_z=3mm (Δt_b=10ps)	
		ΔE_{max}, MeV	P, MW	ΔE_{max}, MeV	P, MW
0.3	40	6.52	253	5	148
	30	4.89	142	3.75	83
	20	3.26	63	2.5	37
0.365	40	9.55	367	7.31	215
	30	7.17	207	5.48	121
	20	4.78	92	3.66	54

The next element where the losses can take place is the coupler. A dominant trapped mode of TM_{010}-type was identified at frequency f_{tr}=8.1GHz from simulations [1]. Analytical calculation of the kinetic energy loss along the train is given in Figure 2. Noticeable frequency detuning f_{tr}/f_b=6.23 prevents from building-up of a resonant trapped field. Average kinetic energy loss over the pulse length is insignificant (<0.1MeV).

The upstream damper and downstream taper (see [1]) can be analyzed with a similar analytical approach as the regular dielectric. The SiC absorber with ε=13.2 and tgσ=0.20 has a 12mm regular length and an 18mm long taper (from 2a=12mm to 14.5mm ID). The main difference is that bunches radiate independently, without space-time building-up of the field. There are three reasons of that: i) drain time for the damper and tapers is much less than the inter-bunch interval; ii) low Q-factor of the damper reduces dramatically the wake attenuation length $S_{w\ att.}=\lambda Q|\beta-\beta_{gr}|/\pi$; and iii) tapering and strong attenuation result in decoherence.

For the regular part of the HOM damper, we have f=11.7GHz, r/Q=5.2kΩ/m, Q=6.5, β_{gr}=0.12 and kinetic energy lost by a 40nC, 3mm bunch is 0.027MeV

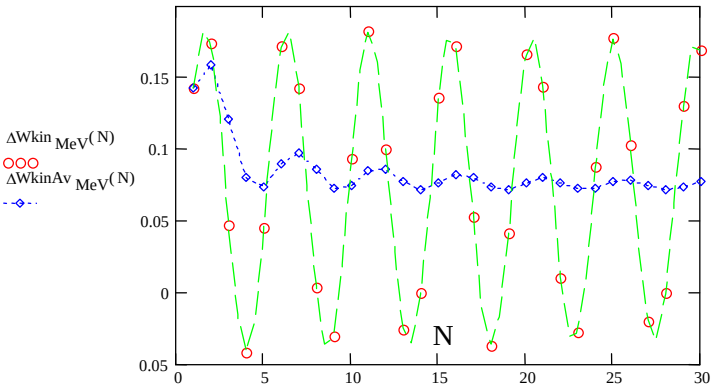

FIGURE 2. Kinetic energy losses (MeV) of different bunches along the train interacting with the dominant mode trapped into the coupler (circles on the dashed line). The losses averaged over the train are shown with diamonds (dotted line)

To estimate the losses in the adiabatic taper it is convenient to apply (3). Indeed, since the local power does not depend on the interaction length, the electrodynamical parameters (including resonant frequency) can be assumed in this formula as corresponding functions on the longitudinal coordinate. Those can be calculated analytically from the boundary problem variations at different dielectric thickness. For instance, near the edge of the damper taper the local parameters are the following: f=30.2GHz, Q=26, r/Q=1.6kΩ/m and β_{gr}=0.62. The losses of kinetic energy integrated over the entire 3cm damper length are ~0.05MeV.

Analogously, one can analyze the dielectric taper. Near the downstream edge of the taper we have f=35GHz, Q=5200, r/Q=1.21kΩ/m, $|\Phi_b|$=0.086 and β_{gr}=0.74. The energy losses integrated over the 21mm taper are ~0.02 MeV. Thus the sum of losses in the tapers and absorber is about 0.09 MeV.

We do not consider here transient (or diffraction) radiation losses from the stopper ring (see [1]) and in the dielectric-to-metal and SiC-to-ceramics transitions. Well-benchmarked analytical diffraction model [9] can be applied with corresponding modifications of the approach [10]. However, the losses are negligibly small due to substantial length of the bunch, smoothed transitions (dielectric thickness is only 0.475 mm on the edge), and proximity to the metal pipe wall. One can expect even smaller diffraction losses in the transitions from regular dielectric to taper and at coupler steps out.

Transverse stability

For the regular part of the rf extraction dielectric tube there are two asymmetric modes: ~14.2GHz for a dipole mode, and ~16GHz for a quadrupole mode. Although the coupler is intentionally symmetrized with two 120° cavities [1], both modes can potentially develop into BBU effect due to the relatively low beam energy and high current, some mode transformation at imperfect transmission in the coupler, beam noise (and/or cumulated displacements in linac – see below), and misalignments. We estimate

here analytically dipole mode effect only, but most of qualitative conclusions can be applied for the quadrupole mode as well.

Since the initial sources of the transverse instability are usually beyond of our control, we will use the threshold current and increment to characterize approximately this collective effect. In general the dipole mode is not matched for both ends of the slow wave system of extractor, and beam pulse length exceeds the doubled filling time for this mode (β_{1gr}=0.434). Hence we can apply the formula derived for single-mode regenerative instability:

$$I_{thr} \approx \frac{m_0 \gamma c^2 / e}{Q_{Loaded}\, r_\perp / Q} \cdot \frac{\lambda_r}{2\pi L^2} \cdot \frac{\beta^2 / \beta_r^{\,2}}{\mathrm{Re}\,\Psi_r \Phi_{1r}(\theta_r) \gamma_r^2 \left(1 - \beta\beta_r + \Xi_r(\beta - \beta_r)\right)}, \qquad (4)$$

where $\Phi_{1r}(\theta_r) = \left(S^2(\theta_r/2) - S(\theta_r)\right)/\theta_r - i2\left(S(\theta_r) - \cos^2(\theta_r/2)\right)/\theta_r^{\,2}$, $S(x) = \sin(x)/x$, $\theta_r = k_r L\left(\beta^{-1}{}_r - \beta^{-1}\right)$ is the phase slippage between the beam and the dipole mode (≈2.61 at maximum increment), $r_\perp$ is the transverse shunt impedance of the structure per unit length (Wilson's definition [11]), Ψ_r is the bunch formfactor with respect to the dipole mode, $\beta = v/c$, $\beta_r = \omega_r'/ck_r$, $\gamma_r = \sqrt{1-\beta_r^2}$, $\Xi_r = Z_0\left(\partial H_{zr}^0/\partial x\right)/\left(\partial E_{zr}^0/\partial y\right)$ is the hybrid coupling coefficient (from the generalized Panofsky-Wenzel theorem accounting the Lorentz' force and slippage [8]).

Note, since $I_{thr} \sim 1/L^2$ and $P \sim (IL)^2$ (see (1) and (2)), the ultimate power limited by regenerative BBU is also inversely proportional to the length squared: $P(I_{thr}) \sim L^{-2}$.

The transverse shunt impedance $r_\perp/Q$=597Ω/m was found from both versions of GdfidL [7] (0.3% difference). Hybrid coupling coefficient Ξ_r≈0.9 was calculated both analytically [8] and from GdfidL (the difference is ~11%). The imperfect reflections from the ends can be taken into account as decreased loaded Q-factor for the dipole mode. In the absence of the damper we assumed here Q_{loaded} ≈1000. The characteristics of the multi-bunch instability are estimated in Table 4. The last column gives the solenoidal magnetic field required to raise the threshold current up to the operating current.

TABLE 4. Regenerative BBU characteristics for dielectric tube L=0.3m, 15MeV, q=40nC (I=52A).

Δt_b, ps	I_{thr}, A (B_z=0)	Increment ν, GHz (B_z=0)	B_z, T (I_{thr}=52A=I)
10	12	0.15	0.78
6.7	9.6	0.2	0.97

One can see the increments are only by 6.6-8.7 times less than the bunch sequence frequency and simultaneously the threshold currents are noticeably less than the operating current 52A. It represents a serious likelihood of the instability. For comparison: in the 21GHz experiment we had I≈17A (39MeV, 275nC train) and I_{thr}≈8.4A, ν=0.06GHz increment at Q_{loaded} ≈1000, and σ_z≤1mm. Under these conditions the rise time is about the same as the pulse length. Analysis of experimental results indicated several signs of development of transverse instability [1].

We can increase the regenerative threshold current by substantial reduction of loaded Q-factor of the dipole mode with damping load. The load reduces only the upstream reflection coefficient Γ_1, whereas the downstream reflection coefficient Γ_2 (from coupler) remains very close to unity. Estimation of the corresponding external Q-factor determined by the end reflections is the following [8]:

$$\frac{-L\,\omega_r'/c}{\left|\beta_{1gr}\right|\ln\left|\Gamma_1\Gamma_2\right|} \le Q_e < \frac{L\,\omega_r'/c}{\left|\beta_{1gr}\right|\left(1-\left|\Gamma_1\Gamma_2\right|\right)} \tag{5}$$

For the two-resonator SW driver linac the corresponding characteristics are very different. The estimated resonant dipole mode frequency is about 1.6GHz, $r_\perp/Q$=271Ω/m, resonator length L≈1m, and β_{1gr}=0.041. Since the group velocity is very small, and the beam pulse is short (compared to $2L/c\beta_{1gr}$), the effect of the reflections from the ends is negligible because this is stored energy mode of beam interaction with the transverse collective wake. Under these SW conditions the effective Q-factor in (4) is essentially the same as unloaded Q-factor for the SW dipole mode (Q≈14860 found from GdfidL code). The same formally follows from (5): since the linac structure is a cavity, $\Gamma_1\Gamma_2\to1$, and $Q_e\to\infty$. Although the resulting threshold current is low (about 1A or even less), the increment is low as well (~0.023GHz for 40nC bunches) due to very high quality factor of each cell. So the rise time exceeds the pulse duration. In the absence of BBU the linac can still act as an initial source of transverse beam modulation: it will amplify any transverse perturbation occurred in the injector or linac. More detailed analysis may be required such as end-to-end time-domain 3D self-consistent beam simulations with inclusion of the longitudinal dynamics.

SINGLE-BUNCH MODE AND BEAM TRANSPORT

Peak power (3) generated by a single bunch does not depend on detuning and dielectric length (as long as the drain time is long enough compared to the RF period). For a 100nC, 10ps (σ_z=3mm) bunch we can obtain P_{1b}=77 MW. No adjustment of resonant linac frequency is necessary. The pulse length is proportional to the regular dielectric length L and is equal to the drain time Δt=2.8ns (≈43 rf cycles) for L=30cm. Beam loading causes additional energy spread due to energy loss of trailing particles in the bunch. The maximum loss is ΔE_{max}=3.5MeV, and the energy loss averaged over the bunch is ΔE_{av}≈2.15MeV.

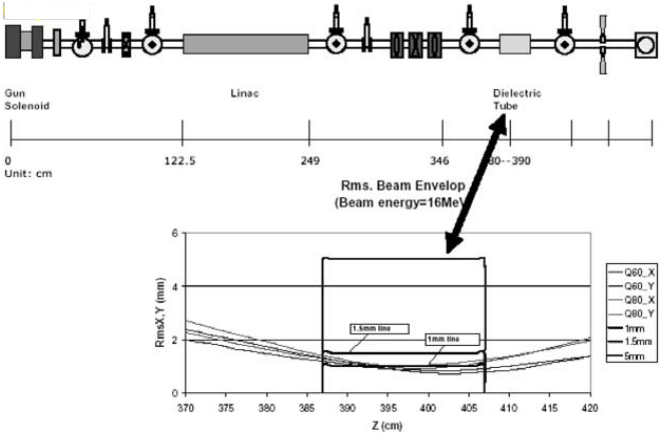

FIGURE 3. Beam line scheme and r.m.s. beam envelops in AWA and extractor simulated with PARMELA at E=16MeV, Q=60-80nC.

The upgraded AWA facility presents a unique opportunity to exceed 100MW peak power in the single-bunch mode for a short enough bunch. For instance, assuming σ_z=2mm (6.7ps), q=100nC we have: P_{1b}=131 MW, ΔE_{max}=4.5MeV, and ΔE_{av}=3.7MeV.

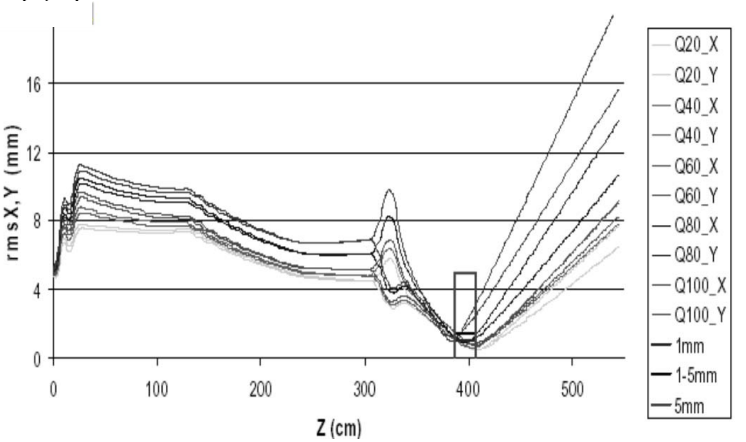

FIGURE 4. R.M.S. envelops at E=19MeV Q=20-100nC.

Single-bunch transport was simulated with PARMELA code from the cathode to the downstream end of the extractor at different bunch charges (see Figure 4). Although these simulations do not take into account wakefield effects, they demonstrate a very good acceptance of the accelerator and beam optics to accommodate individual bunches up to 100nC.

REFERENCES

1 A. V. Smirnov, D. Yu, "15.6 GHz Ceramic RF Power Extractor Design", these proceedings.
2 D. Yu, D. Newsham, A. Smirnov, in Proc. 10th Advanced Accelerator Concepts Workshop, AIP 647, pp. 484-505, 2002.
3 D. Newsham, A. Smirnov, D. Yu, W. Gai, R. Konecny, W. Liu, H. Braun, G. Carron, S. Doebert, L. Thorndahl, I. Wilson, W. Wuensch in Proc. of 2003 Part. Acc. Conf., Portland, Oregon, May 12-16 (2003) 1156.
4 M.E. Conde, in Proc. 10th Advanced Accelerator Concepts Workshop, AIP 647, pp. 63-69, 2002.
5 M.E. Conde, W. Gai, C. Jing, R. Konecny, W. Liu, J.G. Power, H. Wang, Z. Yusof, in Proc. of 2003 Part. Acc. Conf., Portland, Oregon, May 12-16 (2003) 2032; The Argonne Wakefield Accelerator: Facility; See http://127.0.0.1:1025/js.cgi?pcaw&r=15573.
6 J. G. Power, W. Gai, R. Konecny, C. Jing, W. Liu, S. H. Gold, A. K. Kinkead, in Proc. of 2003 Part. Acc. Conf., Portland, Oregon, May 12-16 (2003) 492.
7 Warner Brunes, GdfidL v. 1.8: Syntax and Semantics, March 13, 2002; see http://www.gdfidl.de.
8 A. V. Smirnov. Ph.D. Dissertation, Moscow, MEPhI (1985).
9 A. Smirnov, D. Yu, in the Proc. of 2003 Part. Acc. Conf., Portland, Oregon, May 12-16 (2003) 3171.
10 A.V. Smirnov, D. Yu, in Proc. of the 2001 Part. Acc. Conf., Chicago, (2001) 2994.
11 P. Wilson, High Energy Electron Linac: Applications to storage Rings RF Systems and Linear Colliders, Preprint SLAC-PUB-2884, November (1991).